SHORT COMMUNICATION

Contributions intended for publication under this heading should be expressly so marked; they should not exceed about 1000 *words; they should be forwarded in the usual way to the appropriate Co-editor; they will be published as speedily as possible.*

Acta Cryst. (1992). B**48**, 546–548

Temperature-dependent space-group transitions in crystals of guanylate kinase from yeast.

By THILO STEHLE and GEORG E. SCHULZ,* *Institut für Organische Chemie und Biochemie der Universität, Albertstrasse* 21, 7800 *Freiburg im Breisgau, Germany*

(*Received* 8 *January* 1992; *accepted* 25 *March* 1992)

Abstract

The structure of guanylate kinase from baker's yeast has been solved at low resolution in an orthorhombic crystal form that is closely related to the tetragonal form previously determined at high resolution. The two crystal forms grow in the same drop. Transitions between these crystal forms have been observed in each direction. They can be correlated with temperature changes.

Introduction

Guanylate kinase (GK; ATP:GMP-phosphotransferase; E.C. 2.7.4.8) is a small monomeric enzyme catalyzing the reaction (d)GMP + Mg^{2+}ATP $\rightleftarrows$ (d)GDP + ADP + Mg^{2+}. The protein consists of 186 amino-acid residues; its sequence is known (Berger, Schiltz & Schulz, 1989). The three-dimensional structure of the complex (GK:GMP) between enzyme and GMP substrate in the tetragonal crystal form has been established at 2.0 Å (1 Å = 0.1 nm) resolution (Stehle & Schulz, 1990, 1992); the chain fold is depicted in Fig. 1. The tetragonal crystals were always accompanied by a related orthorhombic crystal form growing in the same drop. The structure of the orthorhombic crystals has now been solved by molecular replacement at low resolution. Here, we report the molecular packing differences between the two crystal forms.

Materials and methods

Crystallization and data collection

All crystals were grown at 293 K and pH 5.5 from $(NH_4)_2SO_4$ using the hanging-drop method according to the protocol of Stehle & Schulz (1990). The two crystal forms were obtained in the same drop and could not be visually distinguished from each other. All crystals were mechanically labile. In an extended search for a crystal storage buffer we tried different $(NH_4)_2SO_4$ concentrations, the addition of various organic compounds and the addition of 1 to 3% (*w*/*v*) bovine serum albumin, but the crystals always cracked within minutes. Thus, we mounted the crystals directly from the drops.

* Author for correspondence.

0108-7681/92/040546-03$06.00

The characteristics of the tetragonal crystal form *A* and the orthorhombic crystal form *B* are given in Table 1. Fresh crystals of either form exhibited sharp reflection profiles with a width of 0.2° as defined by the profile above 10% of the maximum. The reflections were significantly broader after a space-group transition had taken place (see below). The unit cells share the *c* axis (which in the *B* form is 2.6 Å shorter than in the *A* form) while the *a* and *b* axes of the *B* form correspond to the diagonals in the *A* form (see Fig. 2). The crystal forms were identified by four characteristic reflections, given in Table 1, as well as by the length of the *c* axis.

At 293 K, a native data set was collected from a single *B*-form crystal (1100 × 650 × 400 μm) using Ni-filtered Cu $K\alpha$ radiation on a four-circle diffractometer (model

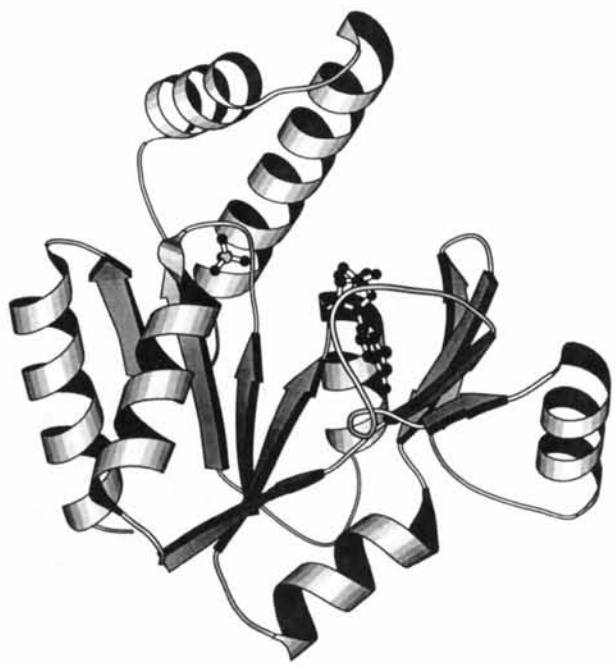

Fig. 1. Ribbon drawing of the refined model of guanylate kinase ligated with GMP obtained using the program *MOLSCRIPT* (Kraulis, 1991). GMP and a bound sulfate ion are shown as ball-and-stick models.

Table 1. *Comparison of the tetragonal and orthorhombic crystal forms of guanylate kinase ligated with GMP*

	Form *A*	Form *B*
Space group	$P4_12_12$	$C222_1$
a (Å)	50.8	71.2
b (Å)	50.8	72.3
c (Å)	155.3	152.7
Enzyme molecules/asymmetric unit	1	2
Diffraction limit (Å)	2.0	Better than 3.0
Data collection (Å)	∞ to 2.0	∞ to 5.9
Characteristic reflection difference[a]		
0,0,14 (0,0,14)	Extinct	Strong
030 (330)	Extinct	Strong
0,10,0 (10,10,0)	Strong	Weak
0,10,1 (10,10,1)	Weak	Strong
No. of crystals at 281 K[b]	33	1
No. of crystals at 293 K	30	36

Notes: (*a*) The *hkl* values are from crystal form *A*; the *hkl* of form *B* are given in parentheses. (*b*) Native and derivative guanylate kinase crystals were analyzed on precession cameras at 293 K and/or on a four-circle diffractometer at 281 or 293 K. Only unambiguously classified crystals were taken into account. No intermediates between the two crystal forms were observed. Only one 7° precession photograph showed an intermediate pattern which, however, is likely to result from a transition during the exposure.

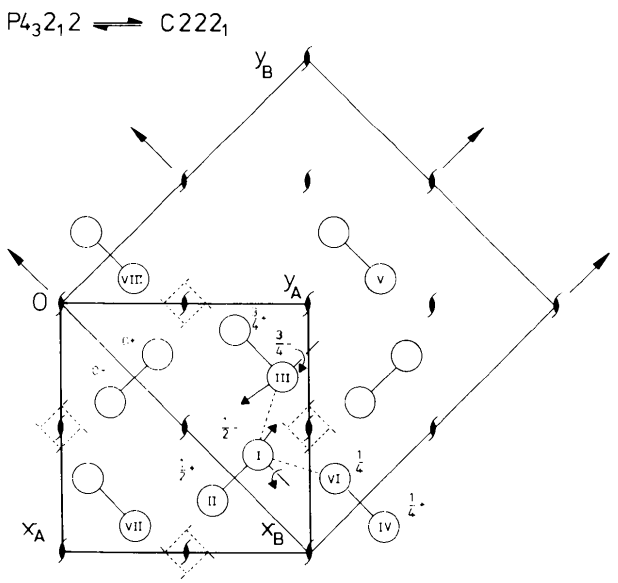

Fig. 2. Relationship between the lattices of crystal forms *A* and *B* which belong to space groups $P4_32_12$ and $C222_1$, respectively. The tetragonal and orthorhombic unit cells are drawn in thick and thin lines, respectively (common origin at 0). For simplicity, the small differences in axial length of form *B* have been neglected. The 2_1 symmetries apply to both forms while the 4_3 symmetries (dashed lines) deteriorate upon *A* to *B* transition. The tight crystal contacts linking molecules (I) and (II) (Table 2) and equivalents are represented by a solid line. The arrows indicate rotations and translations during the *A* to *B* transition. Contact (I)–(II) opens up to some extent but keeps its symmetry. All other contacts become asymmetric. The symmetry reduction can be visualized with contacts (I)–(III) and (I)–(VI) (dashed lines) which are part of a 4_3 ladder and thus identical in form *A*, but different in form *B*.

$P2_1$, Nicolet/Siemens) and the procedure of Thieme, Pai, Schirmer & Schulz (1981). Scan range and speed were 0.8° and 2.5° min^{-1}, respectively. Before data collection the crystal had been measured for 3 days in its *A* form on the same machine. Subsequently, it had undergone a space-group transition, which in fact was the second of the two directly observed transitions described below. The data set obtained consisted of all 1153 reflections with indices $h \geq 0$, $k \geq 0$ and $l \geq 0$ in the resolution range ∞ to 5.9 Å. In spite of radiation damage and the transition, we found $R_{F,\mathrm{int}} = 2\Sigma|F_{hkl} - F_{hk\bar{l}}|/\Sigma(F_{hkl} + F_{hk\bar{l}})$ to be as low as 2.5%.

The diffraction-pattern differences between crystal forms *A* and *B* were quantified by comparing the reflection sets ($h \geq k$, $k \geq 0$, $l \geq 0$) and ($h \leq k$, $k \geq 0$, $l \geq 0$) of form *B* with the *A*-form data set. The R_F values in the resolution range ∞ to 5.9 Å were 36 and 28%, respectively; the corresponding correlation coefficients were +0.81 and +0.88. As an additional approach to measuring the change, we calculated the deviation from symmetry within the crystal *B* form. This yielded an R_F value of 43% and a corresponding correlation coefficient of +0.60 for the 479 *hkl*/*khl* reflection pairs ($h \neq k$) out to 5.9 Å resolution. These values indicate that the diffraction patterns and thus also the molecular packings are closely related to each other.

Structure determination

Given the close relationship, we took the structurally well known molecules (I) and (III) of crystal form *A* (Stehle & Schulz, 1992), which are described by the symmetry operators (*x*, *y*, *z*) and ($y - \frac{1}{2}$, $-x + \frac{3}{2}$, $z + \frac{1}{4}$), and transformed them to form *B* using $x_B = (x_A + y_A)/2$, $y_B = (y_A - x_A)/2$, $z_B = z_A$. These two molecules constitute the asymmetric unit of form *B* and represent the initial structure model. The initial *R* factor between calculated and observed structure factors (resolution range 10–5.9 Å) was 48.9%.

Rigid-body refinement

A rigid-body refinement was carried out in the resolution range 10–5.9 Å using the respective option of program *XPLOR* (Brünger, Kuriyan & Karplus, 1987; Brünger, 1990). An initial refinement of 50 cycles treating the two monomers as separate rigid bodies reduced the *R* factor to 40.2%. A further 50 cycles of refinement were then carried out treating the following 15 parts of each molecule as separate rigid entities: residues 0–10, 11–23, 24–55, 56–66, 67–74, 75–81, 82–91, 92–101, 102–114, 115–124, 125–134, 135–141, 142–169, 170–186 and GMP (0 stands for the acetyl group). The refinement finally converged at an *R* factor of 32.1%.

Results and discussion

Space-group transitions

Table 1 shows significantly different crystal form frequencies at 281 and 293 K indicating temperature dependence. At 281 K, all but one of the crystals analyzed belonged to crystal form *A*, whereas crystal forms *A* and *B* were equally present at 293 K. Further evidence came from two cases where temperature changes during data collec-

tion obviously induced space-group transitions. In the first case, an 11° precession photograph taken at 293 K showed a native crystal as being of form *B*. The same crystal was then exposed to X-rays at 281 K on a diffractometer, showing reflection widths of 0.4° and unit-cell dimensions and characteristic reflections of the crystal form *A*. In the second case, diffractometer data of a native *A*-form crystal were collected at 281 K where the reflection width was 0.2°. When after 3 days of data collection the temperature was accidentally raised to 293 K, the crystal changed to the *B* form enabling us to collect the low-resolution data set of the crystal *B* form described above. Concomitantly, the reflections had significantly broadened to a width of 0.4°.

Raising or lowering the temperature, however, did not always induce a space-group transition. Several attempts to collect additional native data of the crystal *B* form failed because of severe radiation damage problems.

Changes in atomic structure and molecular packing

The changes introduced by the rigid-body refinement were quantified by calculating the polar rotation angles and the translation vectors (program *XPLOR*; Brünger, 1990). Superimposing all C_α-atom pairs of the initial molecule (I) and the refined one yielded an residual r.m.s. deviation of 1.0 Å; the polar rotation angle (Rossmann & Blow, 1962) and the translation vector were 2.7° and (−0.13, 0.69, 0.37 Å), respectively. The corresponding values for molecule (III) are 0.9 Å, 2.8° and (−0.23, −1.22, −0.67 Å). The movements of both molecules are indicated in Fig. 2. Subsequently, we calculated the relative movements of the $2 \times 15 = 30$ segments into which the two molecules had been subdivided. For this purpose we superimposed the 30 segments (C_α atoms) of the initial molecules separately with those of the refined ones. The resulting average polar rotation angles and translation vectors were 4.1° (maximum = 6.2°) and 1.4 Å (maximum = 2.2 Å), respectively, indicating that no gross intrinsic structural changes had occurred. Such changes are to be expected in the group of nucleoside monophosphate kinases (Schulz, Müller & Diederichs, 1990).

The observed rotations and translations show that the packing changes accompanying the transitions are small. The *A*-form crystal contacts (Stehle & Schulz, 1992) are the same as those of the *B* form (Table 2). Even the buried surface areas (program *DSSP*, Kabsch & Sander, 1983) of the contacts are similar, except for the largest contact (I)–(II) which has decreased by about 25% in form *B*. Upon transition, molecules (I) and (II) change their position slightly opening up the mutual contact as indicated in Fig. 2, but maintain the twofold symmetry. In contrast, the fourfold screw symmetry relating molecule (I) to (III), (VI), *etc.* is broken (Fig. 2). Crystal contact pairs (I)–(III)/(I)–(VI), (I)–(IV)/(I)–(VII) and (I)–(V)/(I)–(VIII) (Stehle & Schulz, 1992) which are identical in form *A* become asymmetric in form *B*. The rigid-body refinement introduced only a few bad contacts between molecule (I) and its seven neighbors. Six non-H-atom pairs are 1–2 Å apart, and 30 more distances are in the range 2–3 Å. Among them are four hydrogen bonds. A similar calculation for the high-resolution structure of GK (Stehle & Schulz, 1992) yielded five pairs in the range 2–3 Å, three of which were hydrogen bonds.

Table 2. *Changes in molecular packing*

Crystal contact[a]	Buried surface area in form $A^{a,b}$ (Å^2)	Buried surface area in form B^b (Å^2)
(I)–(II)	1020	780
(I)–(III)/(I)–(VI)	340/340	370/300
(I)–(IV)/(I)–(VII)	270/270	240/260
(I)–(V)/(I)–(VIII)	160/160	160/180

Notes: (*a*) The numbering of the crystal contacts and the values for crystal form *A* are taken from Stehle & Schulz (1992). (*b*) Calculated using *DSSP* (Kabsch & Sander, 1983).

Reports on protein crystal-form transitions are not very frequent. A temperature-dependent space-group transition (from $P2_12_12$, $c = 69.2$ Å to $P2_12_12_1$, $c = 140.2$ Å) has been described for crystals of δ-crystallin (Mylvaganam, Slingsby, Lindley & Blundell, 1987). After the transition, the crystals became very radiation sensitive and diffracted only to 6 Å resolution. Moreover, crystals of t-RNA^{Asp} exist in two interconvertible orthorhombic crystal forms with slightly different cell dimensions. The interconversion is probably temperature dependent (Huong, Audry, Giegé, Moras, Thierry & Comarmond, 1984). Another interconversion between two crystal forms has been reported by Dreusicke & Schulz (1988) for cytosolic adenylate kinase from porcine muscle. It is induced by changes of pH and other solvent properties.

In the case reported here, the crystal shrinks along the *c* axis by about 2% during the transition from crystal form *A* to crystal form *B*. Concomitantly, the reflection width increases from 0.2 to 0.4°. It is remarkable that this transition does not disrupt the crystal and does not destroy its diffraction power. Furthermore, the observed transition reflects the lability of the crystal packing which in turn corresponds to the mechanical sensibility of the crystals and the failure to find any enzyme-free storage buffer.

This work was supported by the Deutsche Forschungsgemeinschaft and by the Graduiertenkolleg Polymerwissenschaften.

References

BERGER, A., SCHILTZ, E. & SCHULZ, G. E. (1989). *Eur. J. Biochem.* **184**, 433–443.
BRÜNGER, A. T. (1990). *XPLOR Manual.* Version 2.1. Yale Univ., New Haven, USA.
BRÜNGER, A. T., KURIYAN, J. & KARPLUS, M. (1987). *Science*, **235**, 458–460.
DREUSICKE, D. & SCHULZ, G. E. (1988). *J. Mol. Biol.* **203**, 1021–1028.
HUONG, P. V., AUDRY, E., GIEGÉ, R., MORAS, D., THIERRY, J. C. & COMARMOND, M. R. (1984). *Biopolymers*, **23**, 71–81.
KABSCH, W. & SANDER, C. (1983). *Biopolymers*, **22**, 2577–2637.
KRAULIS, P. J. (1991). *J. Appl. Cryst.* **24**, 946–950.
MYLVAGANAM, S. E., SLINGSBY, C., LINDLEY, P. F. & BLUNDELL, T. L. (1987). *Acta Cryst.* **B43**, 580–582.
ROSSMANN, M. G. & BLOW, D. M. (1962). *Acta Cryst.* **15**, 24–31.
SCHULZ, G. E., MÜLLER, C. W. & DIEDERICHS, K. (1990). *J. Mol. Biol.* **213**, 627–630.
STEHLE, T. & SCHULZ, G. E. (1990). *J. Mol. Biol.* **211**, 249–254.
STEHLE, T. & SCHULZ, G. E. (1992). *J. Mol. Biol.* **224**, 1127–1141.
THIEME, R., PAI, E. F., SCHIRMER, R. H. & SCHULZ, G. E. (1981). *J. Mol. Biol.* **152**, 763–782.